Chapter 2
Design and Realization of Near-Critical Visualization Experiment

Phase-shifting interferometry is one sub-category of holographic optical measurement methods. Generally, the interferometer system is utilized for the quantitative measurement of density field of a fluid. As in heat transfer field, the density is usually correlated with temperature; therefore, the measurement of temperature field by interferometer system becomes possible [1–3]. Following the previous studies as summarized in Sect. 1.5, the current chapter tries to establish an interferometer system for the visualization of near-critical fluid flow and heat transfer behaviors. The challenging point for the current development is the high pressure through flow system design, which is much more difficult than previous closed chambers. Also, the compromise between the pressure selection and the apparatus design should be considered in laboratory scale investigations.

2.1 Basic Design for Phase-Shifting Interferometry

2.1.1 Fundamentals of Phase-Shifting Interferometry

In an interferometer system, the laser beams are spitted into two: one beam passes through the sample, the other goes through the reference optic passages. The reference beam would be affected by the sample field as the refractive index will be changed under heterogeneous density/temperature field. Then the interferograms of the sample beam and the reference beam will be recorded by a CCD camera for data analysis [1, 2]. Indeed, the interferometer technique has been used since the time of Young's two-slit interferometer. It is only in recent years that the interferometer system became more and more used in thermal-related fields, due to the fast development in precise measurement apparatus and high-speed techniques.

L. Chen, *Microchannel Flow Dynamics and Heat Transfer of Near-Critical Fluid*,
Springer Theses, DOI 10.1007/978-981-10-2784-0_2

2.1.2 *Phase-Shifting Interferometry in Non-intrusive Measurement*

Interferometer system has been widely utilized in optics and physical measurement applications. For example, in fake diagnose, precise measurement experiment, crystal science and engineering, food engineering and other fields, interferometer is used as one strong weapon that is able to tell very small difference of samples in a quantitative way. Interferometer is one non-intrusive method of precise measurement; therefore, it is very useful as it does not affect the sample or target. Those applications mainly fall in optical engineering or material engineering fields. In fluid engineering or thermal field this method is not often seen [3, 4]. Several representative applications of interferometer system as shown in Fig. 2.1, which include the convection measurement, two-phase mixing, diffusion parameter measurement, etc. [3, 5–7].

Mach-Zehnder interferometer is one of the basic measurement kinds among many set-ups of interferometer systems [5]. The Mach-Zehnder interferometer design can be found in Fig. 2.1a: after the generation of laser in the Laser Source

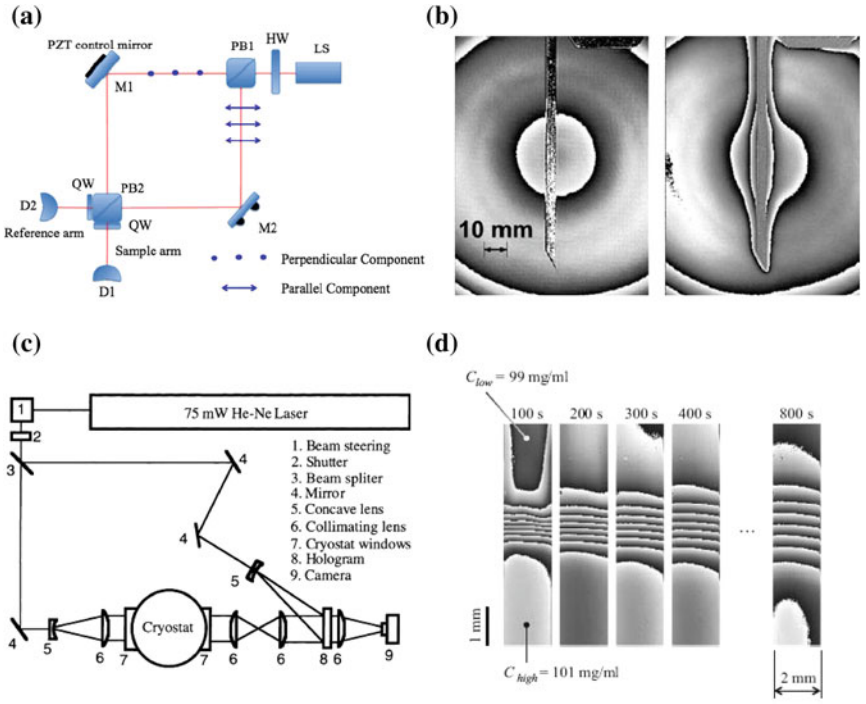

Fig. 2.1 Design and representative applications of interferometer system. **a** Mach-Zehnder interferometer [5]; **b** interferogram of a heated vertical copper plate [6]; **c** Double exposure interferometer [3]; **d** NaCl diffusion in water [7]

(LS), the laser beam goes through a half wave retarder (HW) and beam splitter (PB1) to be separated into a sample beam and reference beam; then the sample beam goes through the sample and interfere with the reference beam and finally be recorded by the detector (D1 and D2). In Fig. 2.1c, another interferometer design is shown (with a similar principal).

2.1.3 Phase-Shifting Interferometry for Near-Critical Fluids

Phase-shifting interferometer system will record the interferograms of the sample beam and reference bean and then recover the field information of the sample. It is important for the fluid sample to have enough phase changes during the passage of the laser beam. Then the data could be proceeded to show the details in a quantitative way [1, 2]. The sample optical path and the reference path would be different due to the refractive index changes of the sample and the reference beam. This refractive index changes may be caused by the temperature, density, pressure or concentration variations in the sample. Therefore, based on the reference value and the quantitative data from the interferometer measurement, the field information could be obtained.

Basically, the refractive index of the sample is directly corrected to the temperature and/or density. The temperature changes δT and the corresponding interferograms could be expressed as [3]:

$$\delta T = \lambda/[(1 - n_0)BL] \tag{2.1}$$

where λ is the wavelength of laser, n_0, B and L indicate the reference refractive index, thermal expansivity and optical path, respectively. For near-critical fluid, the refractive index n_{sup} could be referenced by classical Clausius-Mossotti equation [8]:

$$\frac{\kappa - 1}{\kappa + 2} = \frac{N\alpha}{3} \tag{2.2}$$

and the Lorentz-Lorenz equation [9]:

$$\kappa = n^2 \tag{2.3}$$

where the κ, N and α represent dielectric constant, molecular number per unit volume and polarization constant, respectively.

The right-hand side of Eq. 2.2 is proportional to density; therefore, n_{sup} can be calculated from the following equation:

$$\left(n_{\text{sup}}^2 - 1\right) \Big/ \left(n_{\text{sup}}^2 + 2\right) = \left[\rho_{\text{sup}}\left(n_g^2 - 1\right)\right] \Big/ \left[\rho_g\left(n_g^2 + 2\right)\right] \tag{2.4}$$

Here the n_g, ρ_{sup} and ρ_g represent gas refractivity, critical fluid density and gas density, respectively. Then, the critical fluid refractivity could be calculated from Eq. 2.4.

Indeed, the near-critical fluid properties vary greatly in the critical region, which is very useful as it can induce enough phase changes in very small piece of near-critical fluid (or in a very thin channel even in microscale) [10, 11]. For traditional fluid of water of air, microscale measurement is very difficult as the refractive index is not affected much in microscale. In other method of measurement in near-critical fluid, the non-intrusive ones using interferometer are usually recommended as they will not affect he flow and heat transfer field. As discussed in Sect. 1.3, there is a couple of experimental systems used interferometer in the measurement of near-critical fluids. However, the major experiments are designed for simple closed critical systems. The open systems and more realistic channel flows are not studied. Indeed, the difficulties for measurement of high-pressure through flows make it extremely challenging as the interferometer system needs transparent parts for laser beam. In the current study, the microscale design then added to that difficulty in both fabrication and system set-ups.

2.2 Design of Experimental System

2.2.1 Overall System Set-up

In the non-intrusive experimental visualization experiment, the near-critical fluid flow and heat transfer are examined by an open through flow circulation system and an interferometer system. The general system design is shown in Fig. 2.2.

As discussed in former sections, the visualization of high pressure flows, the phase separation, or particle flows in PIV method, usually have a clear phase interface of trajectory path lines for camera recording [12, 13]. Those methods can obtain the flow phase distribution and deviations in the fluid region, but the field information is difficult to be visualized. For supercritical and near-critical fluids, only closed system has been discussed (in mimi-scale or centi-meter scale; see Table 1.3) and visualized [3, 4, 14–23]. The challenges of microscale near-critical fluid visualization system are: (1) the high pressure requirement for the operation system, especially for through flow system which should be transparent, makes it much more difficult than closed chambers; the high pressure transparent section and the connecting parts with stainless-steel pipes are necessary; (2) in microchannel field, there are several kinds of designs below 0.8 mm (mainly for silicon based

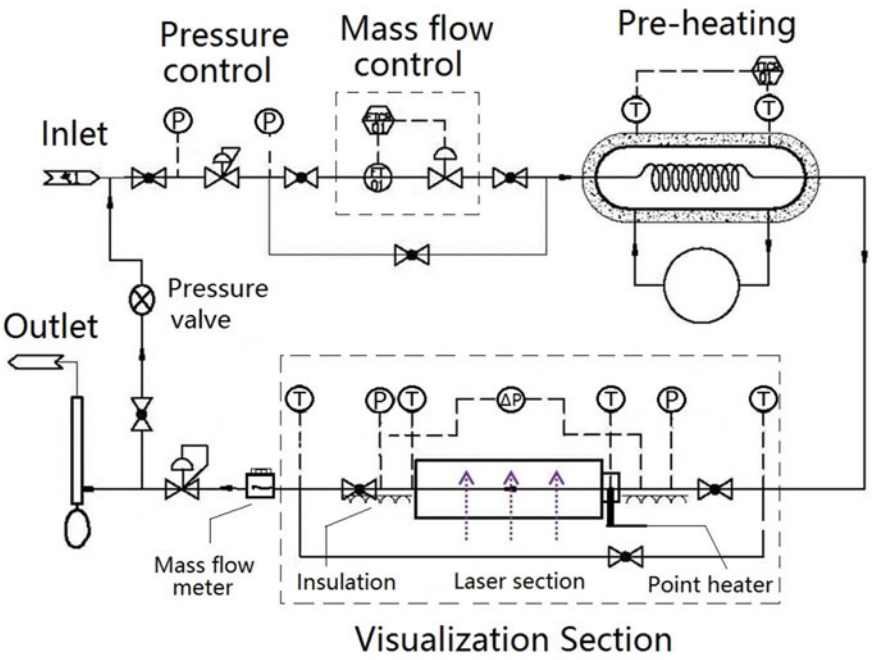

Fig. 2.2 Schematic of the experimental system

channel or metal pipes in small scale), but it is still challenging for the sealing; (3) construction of stable flow system and flow control system as the near-critical fluid is very sensitive to ambient conditions; (4) the calibration of phase-shifting interferometer system.

The current experimental system is consisted of two basic parts: the flow circulation and control system, and the interferometer visualization system. In the flow system, the core part is the transparent microchannel visualization part for the interferometer measurement. Basic target of this experiment is to obtain the basic temperature and density field information under the perturbation or heating inside a microchannel. The fluid through flows inside specifically designed microchannel will go through sub-critical, near-critical and above-critical regions, so as to provide a basic visualization and comparison for the analysis of critical fluids. The basic system design is shown in Fig. 2.2.

As shown in Fig. 2.2, the circulation flow system is consisted of a pressure control panel, a mass flow control panel and a temperature (pre-heating) control part. The liquid fluid first goes through the filter (in this experimental design, high purity fluid is used) and then the pressure is controlled to the design value; then the fluid enters the mass control panel to be regulated to the designed flow rate automatically; after that the pre-heater will increase (or decrease) the fluid temperature before it enters the visualization test section. In the visualization section, a point heater is set at the inlet and the fluid temperature will be affected by a sudden

heating or perturbation from the heating. In the test section, the transparent microchannel is designed and fabricated for laser experiment. Then the fluid flows out of the test section and goes into an accumulating tank, which can be compressed and injected again into the circulation flow.

In the experimental system, a back pressure valve is setup to control the pressure drop inside the flow control section, so as to control the pressure drop inside the microchannel. Precise pressure transducer, pressure-difference transducer, mass flow meter, thermistor and other measurement parts are also set in the experimental framework. The real system picture is shown in Fig. 2.3, which is constructed according to the design in Fig. 2.2.

2.2.2 *Flow System Design and Integration*

The experimental system established in Fig. 2.3 is consisted of integrated pressure control section, flow and temperature control section and data recording section. The front view of the experimental framework is shown in Fig. 2.4a, while the back view of the apparatus is shown in Fig. 2.4b. In Fig. 2.4, the basic arrangement and connections of the compactly designed circulation flow system is shown.

The basic framework of the current design is made of aluminum alloy. The apparatus and test sections are placed in that framework. The total length of the

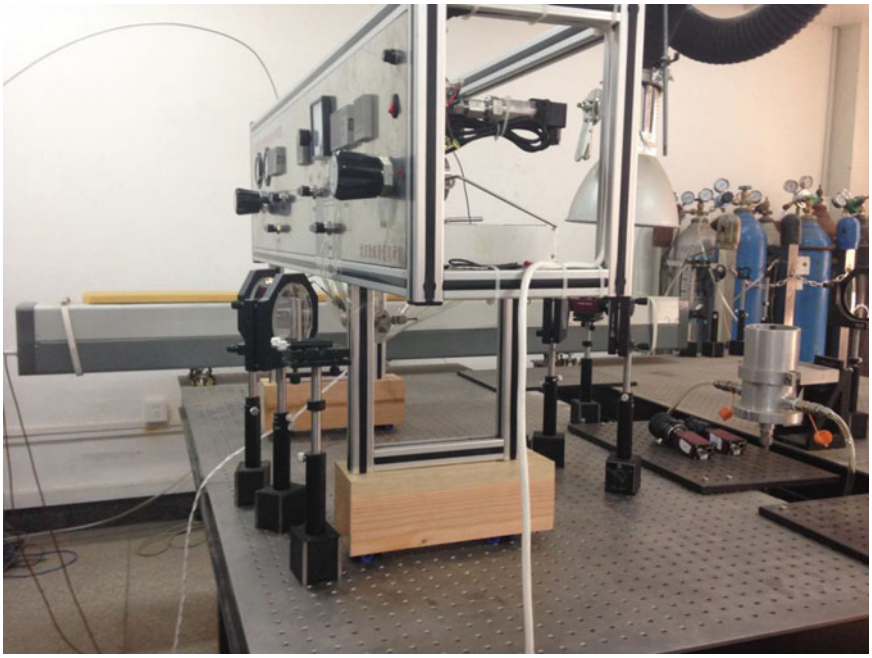

Fig. 2.3 Experimental stage and near-critical flow loop of the experimental system

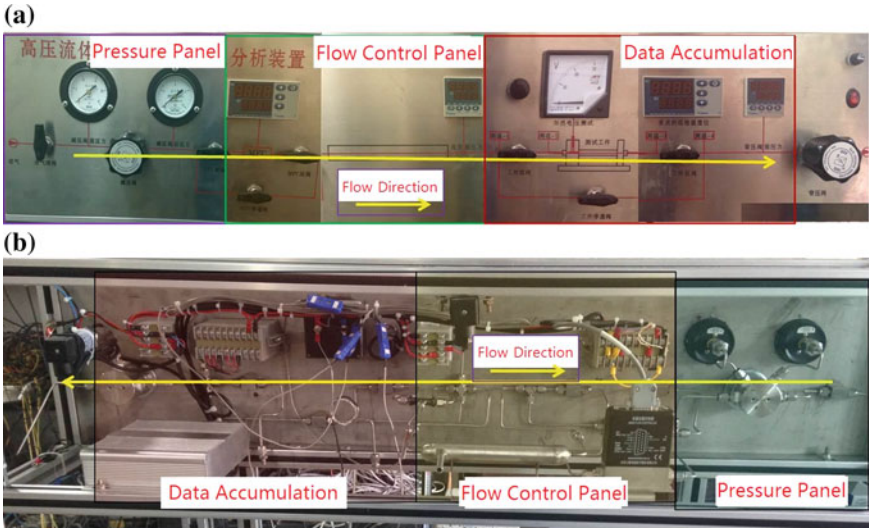

Fig. 2.4 Pictures of the experimental flow system. **a** front view (the control panel); **b** back view (components)

framework is 125 cm, with 25 cm in width and 25 cm in height. A support section is set to make the framework 25 cm higher than the optical stage. The basic circulation flow pipe of the critical fluid is made of stainless steel (022Cr17Ni12Mo2), with an outer diameter of 3.0 mm and inner diameter of 2.0 mm. The major flow pipes and control parts are well insulated during the experiment.

2.2.3 Construction of Flow Components

Indeed, the experimental system of the current study is so designed to minimize the length of flow passages to reduce the friction loss and thermal losses. The main parts are places on the back side of the control panel as shown in Fig. 2.3. Other parts, for example the thermostats, circulation system and heating apparatus are placed on shock pad below the optical stage to minimize the effect from outside.

In the pressure control section, the Xiongchuan series value (SS-8833-F-2) is used, while the back pressure value is SS-9833-F-1 series. In the flow rate control section, the automatic flow rate moderator XHD-MFC-01 is used, which controls the flow rate by a flow rate feedback-control system. In the pre-heating section, a thermostat is used by circulating water flows in a counter flow design (the outer diameter of the heat exchanger is 62.3 mm; the curved design makes it possible for effective heating process). The XHD-LX-300 thermostat is used in this section, which has a temperature control range from 5.0 to 50.0 °C, with an accuracy of ±0.1 °C. In the data accumulation section, the temperature, pressure, pressure difference, flow rate, heating parameters are recorded.

In addition, at the inlet region of the microchannel section, a point Ni-Cr heater is set with 0.8 mm outer diameter, which can directly supply continuous or pulse heat to the fluid. The heater is connected to a 0–30 V electric heating source with maximum power of 20.0 W. The control electric circuit is set under series XHD-HT-01 and it shows linear curve in the power-voltage evolution process.

2.2.4 Visualization Part: Microchannel Fabrication

The most challenging part in this experimental design is the visualization part, including the microchannel design. As the pressure of critical fluids is very high and the connection between the transparent microchannel and the circular stainless pipe is very difficult to seal. For interferometric visualization, the microchannel should be made transparent for laser test. The high pressure resistance of the microchannel becomes one critical problem for the experimental design. In the current experiment, several specially fabricated circular quartz channels are utilized. Indeed, such specially designed quartz channels in microscale are ordered directly from factory, making it very critical for the test.

The sealing and connecting part between the microchannel and the flow pipes are shown in Fig. 2.5. As shown in Fig. 2.5, two chambers are designed to hold the

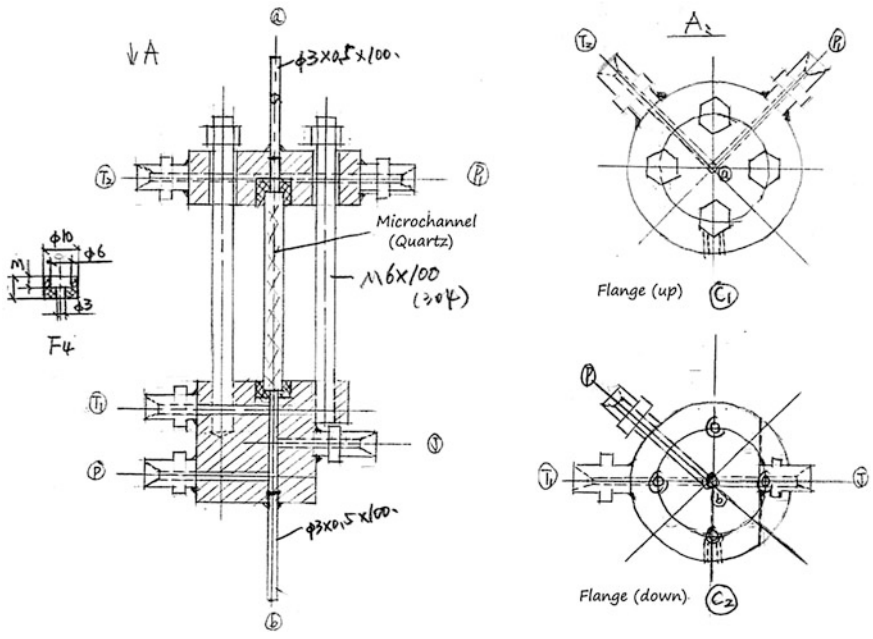

Fig. 2.5 Pressure proof microchannel design

microchannel and connect to the stainless pipes. The microchannel has an outer diameter of 6.0 mm. The PTFE pad is made with proper geometric design to hold the two ends and connects the microchannel to the chamber. During the connection, the PTFE pad is stressed to hold tightly the microchannel ends inside the stainless steel chamber. The chambers are welded to stainless pipes for through flows in the circulation flow system. In the chamber section, heaters, pressure transducers, temperature sensors are also set, as shown in Fig. 2.5. The two chambers are also connected and stressed by an outer holder (made of stainless steel) and fixing bolt, which leaves suitable region of the microchannel for visualization in a proper direction. In the experiment, the whole visualization section is insulated, so as to avoid the ambient effect.

The microchannel design is shown in Fig. 2.6a. The length of the high strength quartz channel is 59.88 mm long with inner rectangular cross section design (3 mm $\times$ 0.3 mm). For the simplicity of fabrication, the channel is initially made in

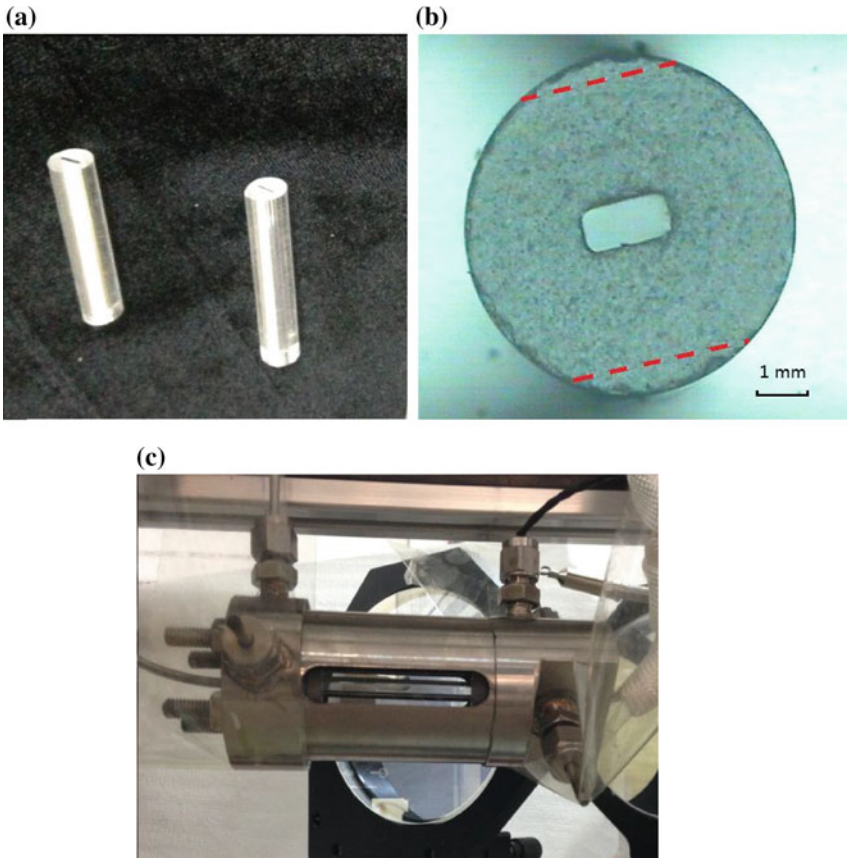

Fig. 2.6 Design of microchannel visualization part. **a** microchannel design and microscopic picture; **b** real configuration of transparent microchannel

a circular outer surface type and then cut to have parallel surfaces align with the inner rectangular designs. In interferometer experiment, the parallel design of the surfaces is very important for the accuracy. Under an accurate microscopic measurement, the microchannel inner cross section size is 3011 μm × 289 μm. Indeed, several other kinds of microchannel designs are also tested in this experiment, but it is very critical for the cross section design and whole size consideration, for both visualization requirement and the pressure bearing capacity.

In the experimental set-up, as shown in Fig. 2.6b, the long thin microchannel is placed in a horizontal direction, with the thin channel cross section set in the vertical direction. Refinement and polishing is made to the microchannel surface to meet the standard of laser experiment after the cutting of the outer surface as shown in Fig. 2.6a. The final structure of the microchannel part is shown in Fig. 2.6b, which is able to sustain a pressure around 5.0 MPa in the tests.

2.3 Optical Design of Phase-Shifting Interferometer

2.3.1 Optical Path

The core part of the phase-shifting interferometer system is the visualization platform design. The visualization is different from the traditional phase surface or PIV methods. It is based on the field information and the interferogram recorded by CCD camera. Phase-shifting is a data process technique associated with interferometer system, which is very useful and capable of much higher resolution than traditional interferometer system [6, 7]. The basic design of Mach-Zehnder interferometer system is shown in Fig. 2.7. The Mach-Zehnder interferometer is very sensitive to perturbations from outside but suitable for the sample setting and measurement.

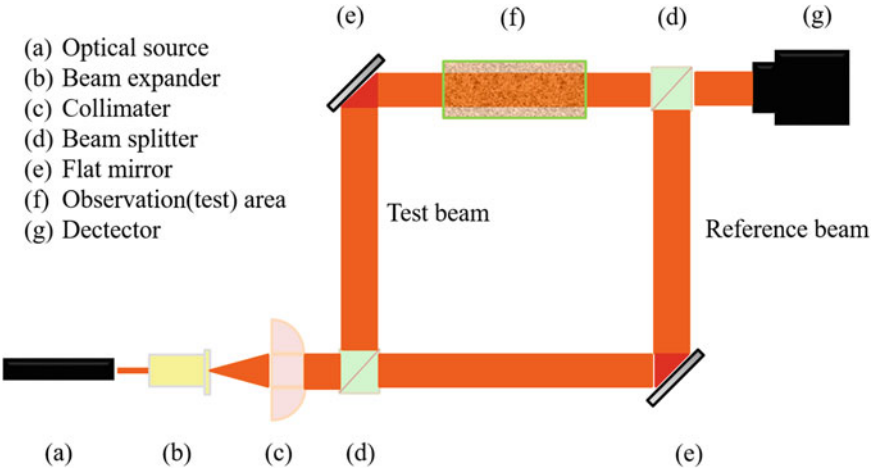

Fig. 2.7 Schematic design of the phase-shifting interferometer system

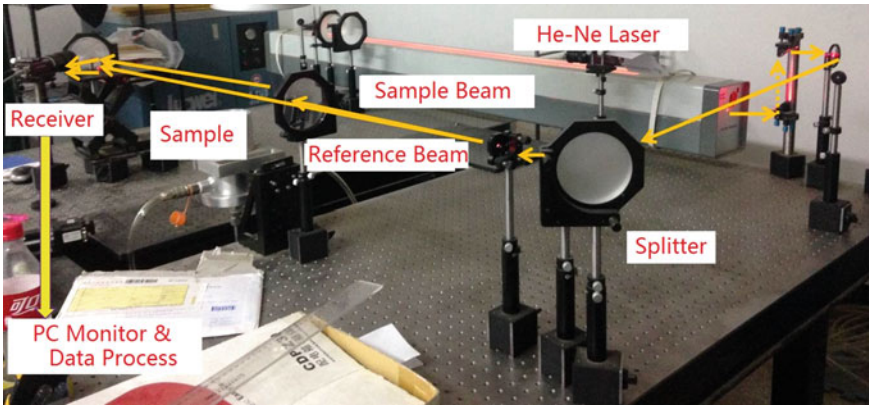

Fig. 2.8 Mach-Zehnder phase-shifting interferometer system

2.3.2 Basic Phase-Shifting Interferometer Set-Ups

The real system construction of the current study is shown in Fig. 2.8. According to the design in Fig. 2.7, basic optical path and flow circulation system are set in the visualization platform. The optical elements are placed in a special platform for visualization experiment. The platform is consisted of two holographic tables (each has a size of 1800 mm × 900 mm). The platform is set 800 mm high and 100 mm thick. The two holographic tables are connected by fixing bolts and have a distance or 275 mm between each other. On the platform, there are bolt-hole arrays with a size distribution of M 6 mm × 26 mm for the fixing of elements. As discussed in former sections, the He–Ne laser beam is generated (λ = 632.8 nm) and paralleled before it goes to the splitter; then the laser is splitted into two beams; one beam goes through the experimental sample, the other is used as reference beam; then the two beams interferences with each other and the interferograms could be recorded by CCD camera for further data process.

2.4 Measurement Procedures

2.4.1 Data Accumulation

The main parameters in this experiment are recorded by CCD camera and sensors. The inlet and outlet temperature, pressure, pressure difference and flow rate of the microchannel are recorded and stored by computer system.

(1) Temperature measurement

Thermocouples are set at the inlet and the outlet of the visualization section to measure the fluid temperature. Also one thermocouple is set at the outlet of the thermostats (each for the cooling fluid and the main working fluid side). The working fluid side is PT100 thermocouple, which is set inside the fluid inlet and outlet. The thermocouples are calibrated in the current experimental ranges with an uncertainty of ±0.1 °C.

(2) Pressure measurement

Pressure sensors are set at the inlet and outlet of the microchannel section. A pressure difference transducer is also set between the inlet and outlet. The ABB 2600T 264G pressure transducer is used in this measurement, with an operation range of 0.6–10 MPa. The pressure difference is measured by ABB 2600T 264D type transducer, the operation range is 0–8 kPa. The pressure transducer has a relative high accuracy with a maximum error of ±0.075 %. The pressure measurement apparatus utilizes 4-20 mA electric data accumulation system and the data is transferred to real pressure values in the computation system.

(3) Mass flow rate

The flow rate control panel has a volume flow rate control range of 0.0–50.0 mL/min. Under the operation pressure below 10.0 MPa, the accuracy of the flow rate measurement is ±0.25 %. The outlet flow rate of the microchannel section is measured by SIEMENS SITRANS FC300 type Coriolis mass flow meter, with a measurement range of 0–350 kg/h. The Coriolis mass flow meter is based on the measurement of Coriolis Effect, and which can measure the mass flow rate accurately in a wide range of parameters. In the current study, the measurement range of 0–4.0 kg/h is selected. The flow meter is consisted of sensor and transducer parts. The accuracy of the current measurement is ±0.1 %.

(4) Interferogram

Besides the temperature, pressure and flow rate measurement, the interferograms are the basic data for the field analysis. In this experiment, the CCD camera (MANTA-MG-504C) is used to record the interferograms. The basic interferogram data then serve as the basic source for the field distribution and evolution analysis.

2.4.2 Uncertainty Analysis

The current experimental system is consisted of the high pressure flow circulation system and the phase-shifting interferometer system. The accuracy of the overall measurement is also dependent on both systems. In the circulation flow system, the measurement error is mainly from the temperature, pressure, pressure difference, and the flow rate measurement. The purity of the working fluid and insulation of the

Table 2.1 Uncertainty of the experimental data

Parameter	Uncertainty
Inlet temperature of test section	±0.1 °C
Inlet temperature of test section	±0.1 °C
Inlet/outlet pressure of test section	±0.075 %
Pressure difference of test section	±0.075 %
Inlet flow rate	±0.25 %
Outlet flow rate	±0.1 %

flow system will also affect the accuracy. In the current study, the high purity working fluid is utilized and well insulation is made to the whole system, especially for the microchannel visualization part, without affecting the interferometer system. The heat loss of the experimental system is estimated to be smaller than 0.1 %, which is a reasonable range as in the previous critical fluid experiments in Tsinghua University has a loss rate of 0.4 % in 0.2 mm outer diameter pipes [24, 25]. In the current study, the high strength quartz microchannel is used, the heat conduction is much smaller than the stainless steel pipe (as used in Refs. [24, 25] for supercritical fluid system), thus to guarantee the insulation and protection. Major experimental uncertainties are listed in Table 2.1 for the current measurement.

For the phase-shifting interferometer measurement system, the platform is places in a special experimental room, which has limited outside light source and noises. All the experiments are conducted in the nights, when the outside effect is limited to its minimum.

In addition, according to the theoretical analysis, the temperature field/density field results can be obtained from Eqs. 2.1–2.4. The relative error can be written as:

$$\frac{\delta(\delta T)}{\delta T} = \sqrt{\left(\frac{\delta B}{B}\right)^2 + \left(\frac{\delta n}{n}\right)^2} \tag{2.5}$$

where B is the thermal expansivity of the fluid, which can be calculated from temperature and pressure measurement. The refractivity n can be calculated by Eq. 2.4 and the measurement of reference point. When the reference point is decided, the relative error of n^2 could be decided by the error of ρ_{sup}. And the ρ_{sup} is dependent on the temperature and pressure measurement. Therefore, the basic error of the calculation should be smaller than ±1.25 % (the pressure measurement error is within ±0.075 %, while the temperature measurement error is within ±0.1 °C).

The measurement uncertainty analysis of experimental data should be done to ensure the present data. In this discussion, basic nomenclatures and definitions described in the "ANSI/ASME Standard on Measurement Uncertainty" are used [26, 27]. In this experimental set-up, the main factors of bias errors are location measurement error and intensity measurement error. The resolution of measured location was approximately 0.01 mm, which corresponds to the real length in one pixel of the bitmap image. The CCD camera detects the density distribution with

precise position (i.e. less than 1pixel measurement error). Therefore, the bias error due to the measurement error of location could be estimated as a value of ±0.03 %, which can be negligible. Concerning the measurement error of intensity, the resolution of detected intensity datum is 0.01 kg/m^3, which corresponds to ±0.27 %. Therefore, the bias error due to intensity measurement is also negligible.

2.4.3 Experimental Procedures

2.4.3.1 Preparations

The preparation of the experiment includes two main parts: one is the high pressure circulation flow system preparation; the other is the calibration of the interferometer system.

(1) Parameters and estimation

Before the experiment, the operation parameter ranges should be checked and estimated/revised for several times. For high pressure experiment, it is specially requested to also make sure the safety equipment is working well in the laboratory. The pressure check should be made several times to make sure it would be reliable under sudden temperature/pressure overshooting, etc. Though the experimental is prepared in closed room, the emergency ventilation and gas processing should also be prepared.

(2) Experimental set-up

Setting-up of the major experimental loop system and the protection apparatus is the main task before the experiment. The thermocouple should be connected with care as the channel size is very small and the contact between the point and the microchannel chamber walls may affect the heat transfer process. Proper space should be kept between each of the panels so as to leave enough room for the insulation and protection apparatus.

(3) Leakage check and injection with N_2

Leakage check should be made after the set-up of experimental system. The high pressure experiment is very dangerous and sensitive for closed loop circulations. In the current experiment, N_2 is injected around 5.0 MPa to be kept under 25.0 °C for 24 h. The pressure drop during this time should be smaller than 0.1 MPa for well sealing of the whole system. In order to avoid the effect of air convection in the experimental room, the microchannel section is covered by a metal box and also a glass cover, leaving the visualization for the laser passage. Also the experimental room is controlled to be within ±0.5 °C to minimize the ambient effect. After the leakage check, the experimental loop is injected with working fluid for several times, so as to clean up the air and N_2. The experimental system is injected and evacuated by using the 99.97 % purity working fluid for more than 3 times.

(4) Calibration with interferometer system

Before the real experiment, the optimal element should be adjusted with its position, height and distribution, to make sure clear and stable interferograms are induced in the receiver plane. The convection of air flow in the experimental room and the test region should be avoided. The optical elements may need to be adjusted for several times before the real experiment.

2.4.3.2 Procedures

(1) Instruments and components check

First, the power source of each measurement panel should be turned on. Then the basic control panel should be checked to show the correct value range. The data from the control panel and the computer recording should be checked and calibrated in this step.

(2) Pressure injection and flow control

The first step is to evacuate and inject of the working fluid for several times to "wash up" the experimental system. After the injection, the pressure and temperature should be checked and recorded for the experimental parameters. During this process, the panels and measurement apparatus should be checked with care to make sure all of them are in good status. The circulation loop flow should be controlled several times by the outlet valve and back up pressure valve. Initially, the flow goes through the side loop, while the pressure is well controlled to the operation range, the microchannel test section could be gradually pressurized. Stable circulation flows should be maintained in this stage for several minutes so as to have a stable initial through flow inside the microchannel. At the same time, the optical system should be adjusted and calibrated to generate suitable interferograms in the receiver CCD camera. The position and height, distribution of the optical elements should be checked to obtain clear and effective results in the measurement. The preparation process may need 60–90 min.

(3) Start-up and data accumulation

In the experiment, the thermostat is firstly started-up to heat up the fluid inside the circulation loop. Then the pressure, temperature and fluid flow rate are monitored and adjusted so as to main a stable flow. Then the CCD camera is started to record the interferogram of the measurement. The point heater is started at designed heating rate. The experimental parameters, including the temperature, pressure, flow rate, will be changed to test the system behaviors under off-design conditions.

(4) Finish of test and clean up

After finishing the data accumulation, the major electric heating source should first be turned down. However, the circulation cooling system should be maintained as

to avoid temperature increase after the heating. When the system temperature recovered to normal range, the flow meter, pressure transducer could be turned down. Then the circulation pump of the thermostat could be closed. Finally, the side flow loop could be open to depressurize the flow system.

References

1. Hecht E (2001) Optics. Addison Wesley Co., New York
2. Lauterborn W, Kurz T, Wiesenfeldt M (2003) Coherent optics, fundamentals and applications. Springer, Berlin
3. Nakano A, Shiraishi M, Murakami M (2001) Application of laser holography interferometer to heat transport phenomena near the critical point of nitrogen. Cryogenics 41:429–435
4. Nakano A, Shiraishi M (2005) Piston effect in supercritical nitrogen around the pseudo-critical line. Int Commu Heat mass Trans 32:1152–1164
5. Pawong C, Chitaree R, Soankwan C (2011) The rotating linearly polarized light from a polarizing Mach-Zehnder interferometer: Production and applications. Opt Laser Tech 43:461–468
6. Shoji E, Komiya A, Okajima J, Maruyama S (2012) Development of quasi common path phase-shifting interferometer for measurement of natural convection fields. Int J Heat Mass Trans 55:7460–7470
7. Torres JF, Komiya A, Shoji E, Okajima J, Maruyama S (2012) Development of phase-shifting interferometry for measurement of isothermal diffusion coefficients in binary solutions. Opt Lasers Eng 50:1287–1296
8. Sommerfeld A (1952) Electrodynamics. Academic Press, London
9. Sommerfeld A (1959) Optics. Academic Press, New York
10. Chen L, Zhang XR, Cao SM, Bai H (2012) Study of trans-critical CO_2 natural convection flow with unsteady heat input and its implications on system control. Int J Heat Mass Trans 55:7119–7132
11. Chen L, Zhang XR, Jiang B (2014) Effects of heater orientations on the natural circulation and heat transfer in a supercritical CO_2 rectangular loop. ASME J Heat Transfer 136:052501
12. Adrian RJ (1991) Particle-imaging techniques for experimental fluid mechanics. Ann Rev Fluid Mech 23:261–304
13. Miyazaki K, Chen G, Yamamoto G, Ohta J, Murai Y, Horii K (1999) PIV measurement of particle motion in spiral gas-solid two phase flow. Exp Therm Fluid Sci 19:194–203
14. Nakano A, Shiraishi M (2005) Visualization for heat and mass transport phenomena in supercritical artificial air. Cryogenics 45:557–565
15. Maekawa T, Ishii K, Ohnishi M, Yoshihara S (2002) Convective instabilities induced in a critical fluid. Adv Space Res 29:589–598
16. Ohnishi M, Yoshihara S, Sakurai M, Miura Y, Ishikawa M, Kobayshi H, Takenouchi T, Kawai J, Honda K, Matsumoto M (2005) Ultra-sensitive high-speed density measurement of the 'piston effect' in a critical fluid. Micrograv Sci Tech 16:306–310
17. Miura Y, Yoshihara S, Ohnishi M, Honda K, Matsumoto M, Kawai J, Ishikawa M, Kobayashi H, Onuki A (2006) High-speed observation of the piston effect near the gas-liquid critical point. Phys Rev E 74:010101 (R)
18. Beysens D, Frohlich T, Garrabos Y (2011) Heat can cool near-critical fluids. Phys Rev E 84:051201
19. Assenheimer M, Steinberg V (1993) Rayleigh-Bénard convection near the gas-liquid critical point. Phys Rev Lett 70:3888

20. Azuma H, Yoshihara S, Onishi M, Ishii K, Masuda S, Maekawa T (1999) Natural convection driven in CO_2 near its critical point under terrestrial gravity conditions. Int J Heat Mass Trans 42:771–774
21. Melnikov DE, Ryzhkov II, Mialdun A, Shevtsova V (2008) Thermovibrational convection in microgravity: preparation of a parabolic flight experiment. Micrograv Sci Tech 20:29–39
22. Beysens D, Chatain D, Nikolayev VS, Ouazzani J, Garrabos Y (2010) Possibility of long-distance heat transport in weightlessness using supercritical fluids. Phys Rev E 82:061126
23. Bartscher C, Straub J (2002) Dynamic behavior of a pure fluid at and near its critical density under microgravity and 1g. Int J Thermophys 23:77–87
24. Jiang PX, Zhang Y, Shi RF (2008) Experimental and numerical investigation of convection heat transfer of CO_2 at supercritical pressures in a vertical tube at low Reynolds numbers. Int J Therm Sci 47:998–1011
25. Zhao CR, Jiang PX, Zhang YW (2011) Flow and convection heat transfer characteristics of CO_2 mixed with lubricating oil at super-critical pressures in small tube during cooling. Int J Refrigerat 34:29–39
26. Japan Society of Mechanical Engineers (1985) Supplement on instruments and apparatus, part 1. Measurement Uncertainty, Maruzen
27. Coleman HW, Steele WG (1989) Experimentation and uncertainty analysis for engineers. Wiley, New York

http://www.springer.com/978-981-10-2783-3

Microchannel Flow Dynamics and Heat Transfer of Near-Critical Fluid

Chen, L.

2017, XXIII, 155 p. 61 illus., 56 illus. in color., Hardcover
ISBN: 978-981-10-2783-3